

Extension of the input-output relation for a Michelson
interferometer to arbitrary coherent-state light sources:
— *Gravitational-wave detector and weak-value amplification* —

Kouji Nakamura¹, and Masa-Katsu Fujimoto²

*Gravitational-Wave Project Office, Optical and Infrared Astronomy Division, National
Astronomical Observatory of Japan, Mitaka, Tokyo 181-8588, Japan*

Abstract

An extension of the input-output relation for a conventional Michelson interferometric gravitational-wave detector is carried out to treat an arbitrary coherent state for the injected optical beam. This extension is one of necessary researches toward the clarification of the relation between conventional gravitational-wave detectors and a simple model of a gravitational-wave detector inspired by weak-measurements in [A. Nishizawa, Phys. Rev. A **92** (2015), 032123.]. The derived input-output relation describes not only a conventional Michelson-interferometric gravitational-wave detector but also the situation of weak measurements. As a result, we may say that a conventional Michelson gravitational-wave detector already includes the essence of the weak-value amplification as the reduction of the quantum noise from the light source through the measurement at the dark port.

Keywords: Gravitational-wave detector, weak-value amplification

1. Introduction

Weak measurements and their weak-value amplifications have been currently discussed by many researchers since their proposal by Aharonov, Albert, and Vaidman in 1988 [1]. In particular, the weak-value amplification has

¹E-mail address: kouji.nakamura@nao.ac.jp

²E-mail address: fujimoto.masa-katsu@nao.ac.jp

been regarded as one of techniques that has been used in a variety of experimental settings to permit the precise measurement of small parameters [2]. This paper is motivated by these researches on the precise measurements in quantum theory.

As well-known, one of typical examples of precise measurements is the gravitational-wave detection. Recently, gravitational waves are directly observed by the Laser Interferometer Gravitational-wave Observatory (LIGO) [3] and the gravitational-wave astronomy has begun. To develop this gravitational-wave astronomy as a precise science, improvements of the detector sensitivity is necessary. So, it is important to continue the research and development of the science of gravitational-wave detectors together with the source sciences of gravitational waves. This paper is also based on such research activities.

Although some researchers already commented that the weak-value amplification might be applicable to gravitational-wave detectors, we have been discussed this issue, seriously. The idea of weak measurements also proposed a new view-point of quantum measurement theory together with an amplification effect. To discuss the application of this idea to gravitational-wave detectors not only leads us to a possibility of exploring a new idea of the gravitational-wave detection but also gives us a good opportunity to discuss what we are doing in conventional gravitational-wave detectors from a different view-point of quantum measurement theory. Therefore, it is worthwhile to discuss whether or not the idea in weak measurements is applicable to gravitational-wave detector from many points of view. In particular, the comparison with conventional gravitational-wave detectors is an important issue in such discussions.

A simple realization of the weak-value amplification is similar to the gravitational-wave detectors in many points. The base of the conventional gravitational-wave detectors is the Michelson interferometer. The arm lengths of this Michelson interferometer are tuned so that the one of the port of the interferometer becomes the “dark port” as we will explain in Sec. 2. Due to the propagation of gravitational waves, photons leak to the “dark port.” The measurement of the photon number at the “dark port” corresponds to the post-selection in weak measurements. This setup is regarded as a measurement of the effective two-level system of the photon. For this reason, we have been concentrated on the researches on weak measurements for two-level systems [4, 5, 6, 7]. In particular, a weak-value amplification in a shot-noise limited interferometer was discussed [5], since the shot-noise is one of important noise in gravitational-wave detectors.

Recently, Nishizawa [7] reported his arguments on the radiation-pressure noise in a weak-measurement inspired gravitational-wave detector. This radiation-pressure noise is also an important noise in gravitational-wave detectors. He also discussed “standard quantum limit,” which is a kind of the sensitivity limit of the detector, and proposed an idea to break his standard quantum limit. Details of the detector model inspired by weak measurements in Refs. [5, 7] will also be explained in Sec. 2. In this detector model, the optical short pulse beam is used to measure the mirror displacement due to gravitational waves, while the continuous monochromatic laser is used for the continuous measurement of the mirror displacement in conventional gravitational-wave detectors. This short-pulse injection is one of ideas in weak measurements proposed by Aharonov et al. [1] and the main difference between a model inspired by weak measurements in Refs. [7] and conventional gravitational-wave detectors. Furthermore, in Ref. [7], arguments are restricted to the situation where the mirror displacement is regarded as a constant in time, while we have to monitor the motion of the mirror displacement by the continuous laser in conventional gravitational-wave detectors. Due to this restriction, we cannot directly compare the results in Ref. [7] with those in conventional gravitational-wave detector and the meaning of “standard quantum limit” in Ref. [7] is not so clear.

To monitor the time-evolution of the mirror displacement is important in gravitational-wave detection, because it corresponds to the monitor of the time-evolution of gravitational waves. Expected gravitational-wave signals are in the frequency range from 10 Hz to 10 kHz. When we apply the detector model in Ref. [7], we may inject femto-second pulses into the interferometer and a sufficiently large number of pulses are used to measure 10 kHz signals. Since we want to continuously measure the time-evolution of gravitational-wave signal in the range 10 Hz-10 kHz, we have to evaluate the averaged data of many pulses, continuously. To accomplish this averaged measurement, the different treatment of the detector in Ref. [7] is required. In conventional gravitational-wave detectors, the response of the detector to gravitational waves is discussed through the input-output relation of the interferometer in the frequency domain in the range of frequencies of gravitational-waves [11]. Therefore, to compare the results with conventional gravitational-wave detectors, it is natural to discuss the input-output relation for the weak-measurement inspired detector model in Ref. [7] taking into account of the time-dependence of the mirror displacement.

In this paper, we regard that the Fourier transformation of optical fields

are averaged variable of many pulses with the time scale which cover the appropriate frequency range and derive the input-output relation for the model in Ref. [7]. The important motivation of this extension is the comparison with the conventional gravitational-wave detectors. To carry out this extension, we have to consider at least two issues. The first issue is in the formulation to describe the input-output relation for the interferometers. In the conventional gravitational-wave detectors, the input-output relations are always derived through the two-photon formulation developed by Caves and Schumaker [8]. However, it is not clear whether or not this two-photon formulation can be applicable to the situation of weak measurements, because the aim of this formulation is to discuss the sideband fluctuations at the frequency $\omega_0 \pm \Omega$ where ω_0 is the frequency of the monochromatic laser and Ω is the frequency of fluctuations around this monochromatic laser. Furthermore, we consider the situation $\omega_0 \gg \Omega$ in the two-photon formulation. It is not clear whether or not the situation $\omega_0 \gg \Omega$ is appropriate for the model in Ref. [7]. We also note that there is little literature in which the input-output relation for gravitational-wave detectors is derived without the two-photon formulation. Therefore, we have to re-derive the input-output relations of gravitational-wave detectors without using the two-photon formulation from the starting point.

The second issue is the extension of the photon state from the light source in the interferometer. In conventional gravitational-wave detectors, the optical field from the light source is in the coherent state whose complex amplitude is given by the δ -function in the frequency domain. On the other hand, the photon state from the light source in the model of Ref. [7] is also a coherent state but its complex amplitude has the broad band support in the frequency domain, which corresponds to the optical pulse. Therefore, we extend the input-output relation for conventional gravitational-wave detectors to the situation where the state of the injected light source is in an arbitrary coherent state. This extension is the main purpose of this paper. As the result of this extension, we can treat the situation of conventional gravitational-wave detectors and that of the model in Ref. [7] from the same input-output relation and compare these models. Furthermore, we can easily see that conventional gravitational-wave detectors already and implicitly includes the essence of the weak-value amplification as the noise reduction from the light source through the measurement at the dark port.

This paper is organized as follows. In Sec. 2, we explain the setup of a simple conventional Michelson gravitational-wave detector and its weak-

measurement inspired version discussed in Ref. [7]. In Sec. 3, we derive the generalized input-output relation which is applicable to the situation where the injected optical beam is an arbitrary coherent state and the derived input-output relation is the main result of this paper. In Sec. 4, we re-derive the conventional input-output relation from our derived extended input-output relation in Sec. 3, which indicates that our extended input-output relation is a natural extension of the input-output relation for conventional gravitational-wave detectors. In Sec. 5, we discuss the situation of the weak-value amplification of the model in Ref. [7] from our derived input-output relation in Sec. 3, which actually realizes the weak-value amplification. Final section, Sec. 6, is devoted to summary and discussion which includes the comparison of the model in Ref. [7] and the conventional Michelson gravitational-wave detector.

2. Michelson weak measurement setup

In this section, we explain the simplest conventional Michelson interferometric gravitational-wave detector and its weak-measurement inspired version discussed in Ref. [7]. The interferometer setup of these two gravitational-wave detectors is described as in Fig. 1. In the setup depicted in Fig. 1, the optical beam from the light source is injected into the interferometer which reaches to the central beam splitter. The central beam splitter separates the optical beam into two paths. We denote these paths as the x -arm and the y -arm, respectively. The separated optical beams propagate along each x - and y -arms, reach to the end-mirrors, and are reflected to the beam splitter by these end-mirrors, again. At the central beam splitter, a part of the reflected beams is returned to the port at which the light source exists. We call this port as the “symmetric port.” The other part of the beam goes to the port at which the photo-detector is prepared as depicted in Fig. 1. We call this port as the “anti-symmetric port.”

To regard the setup in Fig. 1 as a gravitational-wave detector, each end-mirror, which is called x -end mirror and y -end mirror, respectively, undergoes the free-falling motion to the longitudinal direction of the optical beam propagation, respectively. In general relativity, “free-falling motions” are called geodesic motions. The geodesic distance from the beam splitter and each end-mirrors are almost tuned as L . We apply a proper reference frame [9] whose center is the central beam splitter. When gravitational waves propagate through this interferometer, the geodesic distances from the beam splitter to

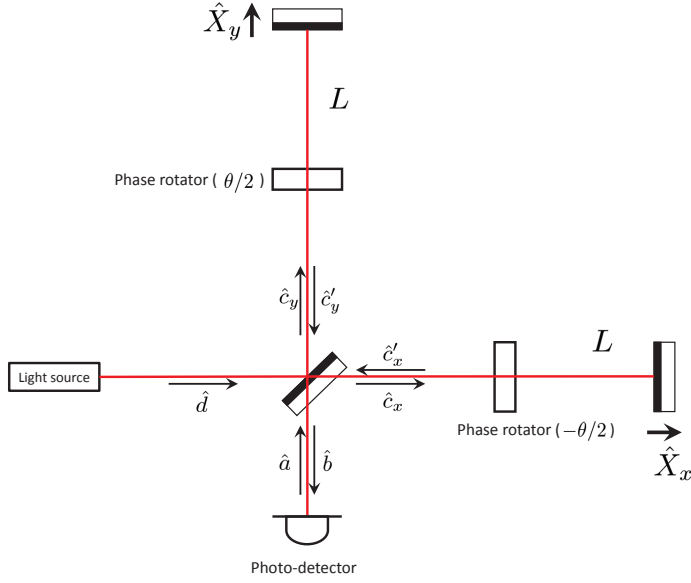


Figure 1: The interferometer setup for the Michelson gravitational-wave detector. The central beam splitter splits the optical beam to the x and y directions and end-mirrors reflect these optical beams to the beam splitter. The geodesic distance from the beam splitter and end-mirrors are almost tuned as L but the mirrors can move this central distance L with tiny distances \hat{X}_x and \hat{X}_y , respectively, along the longitudinal direction of optical beams. Through this setup, we want to measure the effects due to the tiny differential motion of mirrors \hat{X}_x and \hat{X}_y by the photo-detector in the anti-symmetric port. In the conventional Michelson gravitational-wave detector, we inject the monochromatic laser from the light source in this interferometer setup. On the other hand, in the weak-measurement inspired model, we introduce the phase offset $\pm\theta/2$ inspired by the original idea of weak measurements [1]. Furthermore, the injected photon field from the light source to the interferometer is continuous pulse-train in the weak-measurement model. The operators \hat{a} , \hat{b} , $\hat{c}_{x,y}$, $\hat{c}'_{x,y}$, and \hat{d} describe the quadratures for the electric field along the beam line.

each end-mirrors are slightly changed due to the tidal force of gravitational waves. In the proper reference frame, these tiny changes are represented by \hat{X}_x and \hat{X}_y as depicted in Fig. 1. Through this setup of the interferometer, we measure the changes \hat{X}_x and \hat{X}_y due to the gravitational-wave propagation by the photo-detector at the anti-symmetric port. Then, this setup is regarded as a gravitational-wave detector. It is important to note that, if the additional noises other than the gravitational-wave signals are included in these displacements \hat{X}_x and \hat{X}_y , we cannot distinguish the gravitational-wave signals and these additional noises, because we measure the gravitational-wave signal only through the mirror displacement \hat{X}_x and \hat{X}_y . These setup are common both in the conventional Michelson gravitational-wave detector and in the model discussed in Ref. [7].

2.1. Conventional Michelson gravitational-wave detector

In the conventional gravitational-wave detector, L is chosen so that there is no photon leakage at the anti-symmetric port (the phase offset $\theta = 0$ in Fig. 1) when there is no gravitational-wave propagation [10]. For this reason, the anti-symmetric port for the photo-detector is usually called “dark port.” On the other hand, the symmetric port is called “bright port.” As mentioned above, the differential motion $\hat{X}_x - \hat{X}_y$ induced by the gravitational waves leads the leakage of photons to the dark port. This is the signal of the gravitational-wave detection.

In the conventional Michelson interferometric gravitational-wave detector, the state of the electric field from the light source is the monochromatic continuous laser. In quantum theory, this state is characterized by the coherent state with the δ -function complex amplitude with the carrier frequency ω_0 in the frequency domain.

2.2. Weak-measurement-inspired version

Now, we explain the gravitational-wave detector in Fig. 1 from the view point of the standard explanation of weak measurements [7]. The photon states propagate x - and y -arms are denoted by $|x\rangle$ and $|y\rangle$, respectively, and the system to be measured in quantum measurement theory is the which-path information which is a two-level system spanned by the basis $\{|x\rangle, |y\rangle\}$. The difference $\hat{X}_x - \hat{X}_y$, which includes the gravitational-wave signal, is regarded as the interaction strength between the system and the meter variable in quantum measurement theory. We regard that this interaction affects the

photon state at the time $t = t_0$ of the reflection at the end mirrors. The meter variable in this setup is the frequency of photon in the interferometer.

In contrast to the conventional Michelson gravitational-wave detector, we introduce the relative phase offset $\pm\theta/2$ in each arm [10] in the weak-measurement version of this detector. This introduction of the phase offset is inspired by the original idea of weak measurements [1] as explained in Ref. [7]. The weak value amplification occurs when this relative phase offset is approaching to vanishing as discussed in Ref. [1]. Furthermore, we assume that the state of the electric field from the light source is a coherent state whose complex amplitude in the frequency domain has a broad band support, while the δ -function complex amplitude at the carrier frequency ω_0 is used in the conventional gravitational-wave detectors. In other words, in the weak-measurement version, the pulse light is injected into the interferometer instead of the monochromatic laser. This is due to the fact that the meter variable to observe the interaction strength $\hat{X}_x - \hat{X}_y$ is the frequency distribution of photon and the variance of the meter variable should be large in the original idea of weak measurements [1].

Due to the above phase offset θ , the initial state of the photon is given by

$$|\psi_i\rangle = \frac{1}{\sqrt{2}} (e^{i\theta/2}|y\rangle + e^{-i\theta/2}|x\rangle). \quad (1)$$

This state corresponds to the photon state propagating from the central beam splitter to the end mirrors. On the other hand, the initial state of the photon meter variable is given by

$$|\Phi\rangle = \int dp \Phi(p)|p\rangle \quad (2)$$

where p is the momentum, or equivalently photon frequency in the natural unit $c = 1$. The pre-selected state for the total system is $|\psi_i\rangle|\Phi\rangle$. In the situation where the interaction strength $\hat{X}_x - \hat{X}_y =: -g$ is almost constant, the reflection at the end mirrors at the moment $t = t_0$ changes the state of photons through the interaction Hamiltonian

$$\hat{H} = g\delta(t - t_0)\hat{A} \otimes p, \quad (3)$$

where and \hat{A} is the which-path operator

$$\hat{A} := |y\rangle\langle y| - |x\rangle\langle x|. \quad (4)$$

After the interaction (3), we perform the post-selection to the which-path information

$$|\psi_f\rangle = \frac{1}{\sqrt{2}}(|y\rangle - |x\rangle). \quad (5)$$

This corresponds to the detection of the photon at the anti-symmetric port of the interferometer depicted in Fig. 1.

The weak value for this measurement model is given by

$$A_w := \frac{\langle\psi_f|\hat{A}|\psi_i\rangle}{\langle\psi_f|\psi_i\rangle} = -i \cot \frac{\theta}{2}. \quad (6)$$

The final state of the output photon after the post-selection is given by

$$\begin{aligned} |\Phi'\rangle &:= \int dp \Phi'(p) |p\rangle = \langle\psi_f|e^{-ig\hat{A}\otimes p}|\psi_i\rangle|\Phi\rangle \\ &= \int dp \Phi(p) |p\rangle (1 - iA_w gp) + O(g^2). \end{aligned} \quad (7)$$

Evaluating the expectation value of the momentum p under this final state, we obtain

$$\langle p'\rangle - \langle p\rangle \sim 2g \text{Im}A_w (\langle p^2\rangle - \langle p\rangle^2) \quad (8)$$

If we apply the standing point that we want to measure the interaction strength $g := \hat{X}_y - \hat{X}_x$ as a gravitational-wave detector, Eq. (8) shows that the output is proportional to $g \text{Im}A_w \propto g \cot(\theta/2)$. If we consider the situation $\theta \ll 1$, the interaction strength $g := \hat{X}_y - \hat{X}_x$ can be measured by the large factor $\sim 1/\theta$. This is the original argument of weak-value amplification in the case of the imaginary weak value.

The above explanation can easily be extended to multiple photons [7]. The probability distribution for a single photon at the output is given through Eq. (7) as

$$\rho(\omega) := \frac{\langle\omega|\Phi'\rangle\langle\Phi'|\omega\rangle}{\langle\Phi'|\Phi'\rangle}. \quad (9)$$

When the total photon number is N_{out} , the photon-number distribution is simply given by

$$\overline{n(\omega)} = N_{out} \rho(\omega). \quad (10)$$

This implies that the probability distribution $\rho(\omega)$ is regarded as the normalized photon number distribution $f(\omega)$ in the frequency domain defined by [7]

$$f(\omega) := \frac{\overline{n(\omega)}}{N_{out}} := \frac{\overline{n(\omega)}}{\int_0^\infty d\omega \overline{n(\omega)}}. \quad (11)$$

In the Heisenberg picture, the output photon number is given by the expectation value of the number operator $\hat{n}(\omega) = \hat{b}^\dagger(\omega)\hat{b}(\omega)$ through the output annihilation operator $\hat{b}(\omega)$ which is introduced in Fig. 1. This will be discussed in Sec. 5 after derived the input-output relation for the interferometer setup which are applicable to the situation of the weak measurement.

In the understanding of conventional gravitational-wave detectors, the input-output relation for the interferometer plays crucial role [11]. This input-output relation is based on the quantum field theory of the photon field. However, the weak-measurement-inspired version is not described by the conventional input-output relation of gravitational-wave detectors. In this paper, we want to discuss these two typical situation within the same mathematical framework. To carry out this, we have to extend the conventional input-output relation to the situation where the coherent state from the light source has an arbitrary complex amplitude in the frequency domain as shown in the next section.

3. Extension of Input-output relation to arbitrary coherent state

In this section, we derive an extension of the input-output relation of the Michelson gravitational-wave detector, which is depicted in Fig. 1, to an arbitrary coherent state light source in terms of the one-photon formulation. In many literature of gravitational-wave detectors, the two-photon formulation developed by Caves and Schumaker [8] is used. However, as emphasized in Sec. 1, it is not clear whether or not this two-photon formulation is applicable to the situation of the detector model in Ref. [7]. Therefore, we reexamine the derivation of the input-output relation from the starting point. This section is the main ingredient of this paper.

In Sec. 3.1, we describe the notation of the electric field in the interferometer. In Sec. 3.2, we derive the input-output relation of the interferometer in which the photon state from the light source is an arbitrary coherent state. In Sec. 3.3, we summarize remarks on the result in this section.

3.1. Electric field notation

As well known, the electric field operator at time t and the length of the propagation direction z in interferometers is described by

$$\hat{E}_a(t-z) = \hat{E}_a^{(+)}(t-z) + \hat{E}_a^{(-)}(t-z), \quad (12)$$

$$\hat{E}_a^{(-)}(t-z) = \left[\hat{E}_a^{(+)}(t-z) \right]^\dagger, \quad (13)$$

$$\hat{E}_a^{(+)}(t-z) = \int_0^\infty \frac{d\omega}{2\pi} \sqrt{\frac{2\pi\hbar\omega}{\mathcal{A}c}} \hat{a}(\omega) e^{-i\omega(t-z)}, \quad (14)$$

where $\hat{a}(\omega)$ is the photon annihilation operator associated with the electric field $\hat{E}_a(t-z)$, which satisfies the commutation relations

$$[\hat{a}(\omega), \hat{a}^\dagger(\omega')] = 2\pi\delta(\omega - \omega'), \quad (15)$$

$$[\hat{a}(\omega), \hat{a}(\omega')] = [\hat{a}^\dagger(\omega), \hat{a}^\dagger(\omega')] = 0. \quad (16)$$

\mathcal{A} is the cross-sectional area of the optical beam. To discuss the input-output relation of the Michelson interferometer based on one-photon formulation, it is convenient to introduce operator $\hat{A}(\omega)$ defined by

$$\hat{A}(\omega) := \hat{a}(\omega)\Theta(\omega) + \hat{a}^\dagger(-\omega)\Theta(-\omega) \quad (17)$$

so that the electric field (12) is represented as

$$\hat{E}_a(t) = \int_{-\infty}^{+\infty} \frac{d\omega}{2\pi} \sqrt{\frac{2\pi\hbar|\omega|}{\mathcal{A}c}} \hat{A}(\omega) e^{-i\omega t}, \quad (18)$$

where $\Theta(\omega)$ is the Heaviside step function

$$\Theta(\omega) = \begin{cases} 1 & (\omega \geq 0), \\ 0 & (\omega < 0). \end{cases} \quad (19)$$

Due to the property of the Dirac δ -function $\int_{-\infty}^{+\infty} dt e^{i(\omega' - \omega)t} = 2\pi\delta(\omega' - \omega)$, the inverse relation of Eq. (18) is given by

$$\hat{A}(\omega) = \sqrt{\frac{\mathcal{A}c}{2\pi\hbar|\omega|}} \int_{-\infty}^{+\infty} dt e^{i\omega t} \hat{E}_a(t). \quad (20)$$

Therefore, the operator $\hat{A}(\omega)$ includes complete information of the electric field operator $\hat{E}_a(t)$ and is convenient to derive the input-output relation of simple interferometers.

3.2. Input-output relation for the extended Michelson interferometer

In this subsection, we consider the extension of the input-output relation for the Michelson interferometer depicted in Fig. 1. This “extension” includes three meanings. First, the state of the input optical field is unspecified, while that is a coherent state whose complex amplitude is a real δ -function in the frequency domain in conventional gravitational-wave detectors. Second, the tiny motions \hat{X}_x and \hat{X}_y of end-mirrors are not specified within this subsection. Finally, we introduce the phase offset $\pm\theta/2$ for each arm as depicted in Fig. 1. This phase offset is inspired by the original idea of weak measurements [1, 10].

3.2.1. Beam splitter junctions

First, we consider the junction conditions for quadratures at the beam splitter. Following the notation depicted in Fig. 1, the final output electric field $\hat{E}_b(t)$ is given by [12]

$$\hat{E}_b(t) = \frac{1}{\sqrt{2}} \left[\hat{E}_{c'_y}(t) - \hat{E}_{c'_x}(t) \right]. \quad (21)$$

Here, we define

$$\hat{B}(\omega) := \hat{b}(\omega)\Theta(\omega) + \hat{b}^\dagger(-\omega)\Theta(-\omega), \quad (22)$$

$$\hat{C}'_x(\omega) := \hat{c}'_x(\omega)\Theta(\omega) + \hat{c}'_x{}^\dagger(-\omega)\Theta(-\omega), \quad (23)$$

$$\hat{C}'_y(\omega) := \hat{c}'_y(\omega)\Theta(\omega) + \hat{c}'_y{}^\dagger(-\omega)\Theta(-\omega) \quad (24)$$

as in Eq. (17) and the relation (21) is given by

$$\hat{B}(\omega) = \frac{1}{\sqrt{2}} \left(\hat{C}'_y(\omega) - \hat{C}'_x(\omega) \right), \quad (25)$$

Similarly, the electric-field operators $\hat{E}_{c'_y}(t)$ and $\hat{E}_{c'_x}(t)$ are also given by the input fields $\hat{E}_d(t)$ and $\hat{E}_a(t)$ as follows [12]:

$$\hat{E}_{c'_x}(t) = \frac{1}{\sqrt{2}} \left(\hat{E}_d(t) - \hat{E}_a(t) \right), \quad (26)$$

$$\hat{E}_{c'_y}(t) = \frac{1}{\sqrt{2}} \left(\hat{E}_d(t) + \hat{E}_a(t) \right). \quad (27)$$

In terms of the quadrature as in Eq. (17), these relations yield

$$\hat{C}_x(\omega) = \frac{1}{\sqrt{2}} \left(\hat{D}(\omega) - \hat{A}(\omega) \right), \quad (28)$$

$$\hat{C}_y(\omega) = \frac{1}{\sqrt{2}} \left(\hat{D}(\omega) + \hat{A}(\omega) \right), \quad (29)$$

where we defined the operators

$$\hat{C}_x(\omega) := \hat{c}_x(\omega)\Theta(\omega) + \hat{c}_x^\dagger(-\omega)\Theta(-\omega), \quad (30)$$

$$\hat{C}_y(\omega) := \hat{c}_y(\omega)\Theta(\omega) + \hat{c}_y^\dagger(-\omega)\Theta(-\omega), \quad (31)$$

$$\hat{D}(\omega) := \hat{d}(\omega)\Theta(\omega) + \hat{d}^\dagger(-\omega)\Theta(-\omega) \quad (32)$$

as in Eq. (17).

3.2.2. Arm propagation

Next, we consider the retarded effect due to the propagation along each x - and y -arm. Here, each arm length is given by $L = c\tau$, where τ is the retarded time for photons which propagate from the beam splitter to the end-mirrors. In addition to the retarded time τ , the tiny displacement of the mirror \hat{X}_x/c and \hat{X}_y/c also contribute to the phase shift of the electric field. In addition to these retarded effects, we add the retarded time Δt_θ which corresponds to the phase offset $\pm\theta/2$ in Fig. 1. Then, the relations between the electric field $\{\hat{E}_{c'_x}(t), \hat{E}_{c'_y}(t)\}$ and $\{\hat{E}_{c_x}(t), \hat{E}_{c_y}(t)\}$ are given by

$$\hat{E}_{c'_x}(t) = \hat{E}_{c_x}[t - 2(\tau + \hat{X}_x(t)/c) + \Delta t_\theta], \quad (33)$$

$$\hat{E}_{c'_y}(t) = \hat{E}_{c_y}[t - 2(\tau + \hat{X}_y(t)/c) - \Delta t_\theta]. \quad (34)$$

where

$$\frac{\theta}{2} = \omega\Delta t_\theta(\omega). \quad (35)$$

Here, we treat \hat{X}_x/c and \hat{X}_y/c , perturbatively. Through the representation of the electric fields $\hat{E}_{c_x}(t)$ and $\hat{E}_{c'_x}(t)$ as Eq. (18), the relation (33) with

Eq. (35) is given by

$$\begin{aligned}
\hat{E}_{c'_x}(t) &= \int_{-\infty}^{+\infty} \frac{d\omega}{2\pi} \sqrt{\frac{2\pi\hbar|\omega|}{\mathcal{A}c}} \hat{C}'_x(\omega) e^{-i\omega t} \\
&\sim e^{-i\theta/2} \int_{-\infty}^{+\infty} \frac{d\omega}{2\pi} \sqrt{\frac{2\pi\hbar|\omega|}{\mathcal{A}c}} \hat{C}_x(\omega) e^{-i\omega(t-2\tau)} \\
&\quad + e^{-i\theta/2} \int_{-\infty}^{+\infty} \frac{d\omega}{2\pi} \sqrt{\frac{2\pi\hbar|\omega|}{\mathcal{A}c}} \hat{C}_x(\omega) e^{-i\omega(t-2\tau)} \frac{2i\omega \hat{X}_x(t-\tau)}{c}. \quad (36)
\end{aligned}$$

In this expression, \hat{X}_x is regarded as a quantum operator. In this case, there is a ordering problem of the operators \hat{X}_x and $\hat{c}_x(\omega)$, but, here, we keep the order in which the operator \hat{X}_x should be in the right of the operator $\hat{c}_x(\omega)$ at this moment. We note that this ordering problem is harmless within this paper, because we concentrate only on the linear quadrature relations with a coherent state light source.

Here, we introduce the Fourier transformation

$$\hat{X}_x(t) =: \int_{-\infty}^{+\infty} \hat{Z}_x(\Omega) e^{-i\Omega t} \frac{d\Omega}{2\pi}, \quad (37)$$

substitute Eq. (37) into Eq. (36), and take the Fourier transformation (20). Then, we have

$$\begin{aligned}
\hat{C}'_x(\omega) &= e^{-i\theta/2} e^{+2i\omega\tau} \hat{C}_x(\omega) \\
&\quad + e^{-i\theta/2} e^{+2i\omega\tau} \frac{2i}{c\sqrt{|\omega|}} \int_{-\infty}^{+\infty} \frac{d\Omega}{2\pi} e^{-i\Omega\tau} \sqrt{|\omega-\Omega|} (\omega-\Omega) \\
&\quad \quad \quad \times \hat{C}_x(\omega-\Omega) \hat{Z}_x(\Omega). \quad (38)
\end{aligned}$$

Similarly, from Eq. (34), we obtain

$$\begin{aligned}
\hat{C}'_y(\omega) &= e^{+i\theta/2} e^{+2i\omega\tau} \hat{C}_y(\omega) \\
&\quad + e^{+i\theta/2} e^{+2i\omega\tau} \frac{2i}{c\sqrt{|\omega|}} \int_{-\infty}^{+\infty} \frac{d\Omega}{2\pi} e^{-i\Omega\tau} \sqrt{|\omega-\Omega|} (\omega-\Omega) \\
&\quad \quad \quad \times \hat{C}_y(\omega-\Omega) \hat{Z}_y(\Omega) \quad (39)
\end{aligned}$$

through the replacements $\hat{C}'_x \rightarrow \hat{C}'_y$, $\hat{Z}_x \rightarrow \hat{Z}_y$ and $\theta \rightarrow -\theta$ in Eq. (37) and (38).

Substituting Eqs. (38) and (39) into Eq. (25), we obtain

$$\begin{aligned}
& e^{-2i\omega\tau} \hat{B}(\omega) \\
&= i \sin\left(\frac{\theta}{2}\right) \hat{D}(\omega) + \cos\left(\frac{\theta}{2}\right) \hat{A}(\omega) \\
&\quad + \frac{2i}{c} \int_{-\infty}^{+\infty} \frac{d\nu}{2\pi} e^{-i\nu\tau} \sqrt{\left|\frac{\omega-\nu}{\omega}\right|} (\omega-\nu) \\
&\quad \times \left[\left(i \sin\left(\frac{\theta}{2}\right) \hat{D}(\omega-\nu) + \cos\left(\frac{\theta}{2}\right) \hat{A}(\omega-\nu) \right) \hat{Z}_{com}(\nu) \right. \\
&\quad \left. - \left(\cos\left(\frac{\theta}{2}\right) \hat{D}(\omega-\nu) + i \sin\left(\frac{\theta}{2}\right) \hat{A}(\omega-\nu) \right) \hat{Z}_{diff}(\nu) \right], \tag{40}
\end{aligned}$$

where we defined

$$\hat{Z}_{com} := \frac{\hat{Z}_x + \hat{Z}_y}{2}, \quad \hat{Z}_{diff} := \frac{\hat{Z}_x - \hat{Z}_y}{2}. \tag{41}$$

3.2.3. Coherent state of the input optical beam

Eq. (40) indicates that the output operator \hat{B} is given by the operators \hat{A} , \hat{D} , \hat{Z}_{diff} , and \hat{Z}_{com} . In this section, we will see that the \hat{Z}_{diff} and \hat{Z}_{com} are given by \hat{A} and \hat{D} together with the gravitational-wave signal through the equations of motion for end-mirrors, later. Therefore, to discuss the information from the output operator \hat{B} , we have to specify the quantum states associated with the operators \hat{A} and \hat{D} .

The state for the operator \hat{A} is the state which is injected from the anti-symmetric port. On the other hand, the state associated with the operator \hat{D} is the state of the electric field which is injected from the symmetric port. The total state of photon in the output port \hat{B} , i.e., \hat{b} , is determined by the specification of the states for the operators \hat{D} and \hat{A} , i.e, the annihilation operators \hat{d} and \hat{a} . We assume that the state associated with the operator \hat{d} is a coherent state with the complex amplitude $\alpha(\omega)$, the state associated with the operator \hat{a} is vacuum state, and no entangled in these states. Then, the total state $|\psi\rangle$ of photon is given by the direct product of the photon

states of each frequency as

$$\begin{aligned} |\psi\rangle &= \prod_{\omega} |\alpha(\omega)\rangle_d \otimes |0\rangle_a = \prod_{\omega} D_d(\alpha(\omega)) |0\rangle_d \otimes |0\rangle_a \\ &=: D_d |0\rangle_d \otimes |0\rangle_a, \end{aligned} \quad (42)$$

$$\begin{aligned} D_d &:= \prod_{\omega} D_d(\alpha(\omega)) \\ &= \exp \left[\int \frac{d\omega}{2\pi} (\alpha(\omega) d^\dagger(\omega) - \alpha^*(\omega) d(\omega)) \right]. \end{aligned} \quad (43)$$

In the Heisenberg picture, the operator \hat{d} is replaced as

$$D_d^\dagger \hat{d}(\omega) D_d = \hat{d}(\omega) + \alpha(\omega), \quad (44)$$

$$D_d^\dagger \hat{d}^\dagger(\omega) D_d = \hat{d}^\dagger(\omega) + \alpha^*(\omega). \quad (45)$$

In terms of the operator $\hat{D}(\omega)$ defined by Eq. (32), this replacement is equivalent to

$$D_d^\dagger \hat{D}(\omega) D_d = \hat{D}_c(\omega) + \hat{D}_v(\omega), \quad (46)$$

where

$$\hat{D}_c(\omega) := \alpha(\omega)\Theta(\omega) + \alpha^*(-\omega)\Theta(-\omega), \quad (47)$$

$$\hat{D}_v(\omega) := \hat{d}(\omega)\Theta(\omega) + \hat{d}^\dagger(-\omega)\Theta(-\omega). \quad (48)$$

Since we apply the Heisenberg picture, the operator $D_d^\dagger \hat{B}(\omega) D_d$ is useful for evaluation of the photon-number expectation value from the input-output relation (40). We regard the terms $D_d^\dagger \hat{Z}_{com}(\Omega) D_d$ and $D_d^\dagger \hat{Z}_{diff}(\Omega) D_d$ are small correction and we neglect the quadratic terms of these small correction. Operating D_d^\dagger and D_d to Eq. (40), substituting Eqs. (46) into Eq. (40), we obtain the input-output relation as

$$\begin{aligned} &e^{-2i\omega\tau} D_d^\dagger \hat{B}(\omega) D_d \\ &= i \sin\left(\frac{\theta}{2}\right) \hat{D}_c(\omega) + i \sin\left(\frac{\theta}{2}\right) \hat{D}_v(\omega) + \cos\left(\frac{\theta}{2}\right) \hat{A}(\omega) \\ &\quad + \frac{2i}{c} \int_{-\infty}^{+\infty} \frac{d\Omega}{2\pi} e^{-i\Omega\tau} \sqrt{\left|\frac{\omega - \Omega}{\omega}\right|} (\omega - \Omega) \\ &\quad \times \left[i \sin\left(\frac{\theta}{2}\right) \hat{D}_c(\omega - \Omega) D_d^\dagger \hat{Z}_{com}(\Omega) D_d \right. \\ &\quad \left. - \cos\left(\frac{\theta}{2}\right) \hat{D}_c(\omega - \Omega) D_d^\dagger \hat{Z}_{diff}(\Omega) D_d \right]. \end{aligned} \quad (49)$$

This is the most general input-output relation within our consideration. In Eq. (49), the first term in the first line is the leakage of the classical carrier field due to the phase offset $\theta/2$. The remaining terms in the first line is the vacuum fluctuations which corresponds to the shot noise. The second- and third-lines are the response of the mirror motion which includes gravitational-wave signal and radiation pressure noise through the motions of mirrors $D_d^\dagger \hat{Z}_{com}(\Omega) D_d$ and $D_d^\dagger \hat{Z}_{diff}(\Omega) D_d$. The input-output relation (49) is the main results of this paper. To evaluate the input-output relation (49), we have to evaluate $D_d^\dagger \hat{Z}_{com}(\Omega) D_d$ and $D_d^\dagger \hat{Z}_{diff}(\Omega) D_d$ in some way.

3.2.4. End-mirrors' equations of motion (time domain)

In the case of gravitational-wave detectors, $D_d^\dagger \hat{Z}_{com}(\Omega) D_d$ and $D_d^\dagger \hat{Z}_{diff}(\Omega) D_d$ are evaluated through the equations of motions for the end-mirrors. We assume that the mass of the beam splitter and end-mirrors are equal to m . Since we apply the proper reference frame [9] of a local inertia system in which the beam splitter is the center of this coordinate system, \hat{X}_x and \hat{X}_y describe the tiny differential displacement of the geodesic distances of the x - and y -end mirrors from the central beam splitter, respectively. The equations for \hat{X}_x and \hat{X}_y are given by

$$\frac{m}{2} \frac{d^2}{dt^2} \hat{X}_x(t) = \hat{F}_{rp(x)}(t) + \frac{1}{2} \frac{m}{2} L \frac{d^2}{dt^2} h(t), \quad (50)$$

$$\frac{m}{2} \frac{d^2}{dt^2} \hat{X}_y(t) = \hat{F}_{rp(y)}(t) - \frac{1}{2} \frac{m}{2} L \frac{d^2}{dt^2} h(t). \quad (51)$$

where h is the gravitational wave signal which is derived from the tidal force due to the gravitational-wave propagation in the proper reference frame and $m/2$ is the reduced mass of the differential motion of the end-mirrors and the central beam splitter. Furthermore, $F_{rp(x)}$ and $F_{rp(y)}$ are the radiation pressure due to the incident photon.

3.2.5. Radiation pressure forces

The radiation pressure forces in Eqs. (50) and (51) are evaluated through

$$\hat{F}_{rp(x)}(t) = 2 \frac{\mathcal{A}}{4\pi} \left(\hat{E}_{c_x} \left[t - \left(\tau + \frac{\hat{X}_x}{c} \right) + \frac{\Delta t_\theta}{2} \right] \right)^2, \quad (52)$$

$$\hat{F}_{rp(y)}(t) = 2 \frac{\mathcal{A}}{4\pi} \left(\hat{E}_{c_y} \left[t - \left(\tau + \frac{\hat{X}_y}{c} \right) - \frac{\Delta t_\theta}{2} \right] \right)^2, \quad (53)$$

in this paper. The right-hand sides in Eqs. (52) and (53) are just twice of the pointing flux of the electric fields which incident to the end-mirrors, respectively.

Performing the Fourier transformation of the electric field \hat{E}_{c_x} , using Eq. (35), and taking the zeroth- and the linear-order with respect to the operator \hat{X}_x , the radiation-pressure force (52) is given by

$$\begin{aligned} \hat{F}_{rp(x)}(t) &= \frac{\hbar}{c} e^{-i\theta/2} \int_{-\infty}^{\infty} \int_{-\infty}^{\infty} \frac{d\omega}{2\pi} \frac{d\omega'}{2\pi} \sqrt{|\omega\omega'|} \hat{C}_x(\omega) \hat{C}_x(\omega') e^{+i(\omega+\omega')\tau} e^{-i(\omega+\omega')t} \\ &\quad + i \frac{\hbar}{c} e^{-i\theta/2} \int_{-\infty}^{\infty} \int_{-\infty}^{\infty} \frac{d\omega}{2\pi} \frac{d\omega'}{2\pi} \sqrt{|\omega\omega'|} (\omega + \omega') \hat{C}_x(\omega) \hat{C}_x(\omega') \\ &\quad \times \frac{\hat{X}_x(t)}{c} e^{+i(\omega+\omega')\tau} e^{-i(\omega+\omega')t}. \end{aligned} \quad (54)$$

Substituting the Fourier transformation (37) of \hat{X}_x and taking Fourier transformation $\hat{F}_{rp(x)}(\Omega)$ of $\hat{F}_{rp(x)}(t)$, we obtain the expression of the radiation-pressure force which affect to the x -end mirror in the frequency domain as

$$\begin{aligned} \hat{F}_{rp(x)}(\Omega) &:= \int_{-\infty}^{+\infty} dt \hat{F}_{rp(x)}(t) e^{+i\Omega t} \\ &= \frac{\hbar}{c} e^{-i\theta/2} e^{+i\Omega\tau} \int \frac{d\omega}{2\pi} \sqrt{|\omega(\Omega - \omega)|} \hat{C}_x(\omega) \hat{C}_x(\Omega - \omega) \\ &\quad + i \frac{\hbar}{c^2} e^{-i\theta/2} \iint \frac{d\omega}{2\pi} \frac{d\omega'}{2\pi} \sqrt{|\omega\omega'|} (\omega + \omega') \hat{C}_x(\omega) \hat{C}_x(\omega') \\ &\quad \times \hat{Z}_x(\Omega - \omega - \omega') e^{+i(\omega+\omega')\tau}, \end{aligned} \quad (55)$$

where we use the notation $\int = \int_{-\infty}^{+\infty}$ and $\iint = \int_{-\infty}^{+\infty} \int_{-\infty}^{+\infty}$. Similarly, we also obtain

$$\begin{aligned} \hat{F}_{rp(y)}(\Omega) &:= \int_{-\infty}^{+\infty} dt \hat{F}_{rp(y)}(t) e^{+i\Omega t} \\ &= \frac{\hbar}{c} e^{+i\theta/2} e^{+i\Omega\tau} \int \frac{d\omega}{2\pi} \sqrt{|\omega(\Omega - \omega)|} \hat{C}_y(\omega) \hat{C}_y(\Omega - \omega) \\ &\quad + i \frac{\hbar}{c^2} e^{+i\theta/2} \iint \frac{d\omega}{2\pi} \frac{d\omega'}{2\pi} \sqrt{|\omega\omega'|} (\omega + \omega') \hat{C}_y(\omega) \hat{C}_y(\omega') \\ &\quad \times \hat{Z}_y(\Omega - \omega - \omega') e^{+i(\omega+\omega')\tau}. \end{aligned} \quad (56)$$

3.2.6. *End-mirrors' equations of motions (Frequency domain)*

$D_d^\dagger \hat{Z}_{com}(\Omega) D_d$ and $D_d^\dagger \hat{Z}_{diff}(\Omega) D_d$ in the input-output relation (49) are determined by Eqs. (50) and (51) of motions for the test masses in the frequency domain. Multiplying D_d^\dagger and D_d to the Fourier transformed version of Eqs. (50) and (51), we obtain

$$m\Omega^2 D_d^\dagger \hat{Z}_{com}(\Omega) D_d = -D_d^\dagger \hat{F}_{rp(x)}(\Omega) D_d - D_d^\dagger \hat{F}_{rp(y)}(\Omega) D_d, \quad (57)$$

$$\begin{aligned} m\Omega^2 D_d^\dagger \hat{Z}_{diff}(\Omega) D_d &= D_d^\dagger \hat{F}_{rp(y)}(\Omega) D_d - D_d^\dagger \hat{F}_{rp(x)}(\Omega) D_d \\ &\quad + \frac{1}{2} m L \Omega^2 h(\Omega) \end{aligned} \quad (58)$$

from definitions (41) of $\hat{Z}_{com}(\Omega)$ and $\hat{Z}_{diff}(\Omega)$. Here, we have regarded that the gravitational-wave signal $h(\Omega)$ is a classical variable which is proportional to the identity operator in the sense of quantum theory. We also used the displacement operator D_d is time-independent. Equations (57) and (58) indicate that we have to evaluate $D_d^\dagger \hat{F}_{rp(x)}(\Omega) D_d$ and $D_d^\dagger \hat{F}_{rp(y)}(\Omega) D_d$ to evaluate $D_d^\dagger \hat{Z}_{com}(\Omega) D_d$ and $D_d^\dagger \hat{Z}_{diff}(\Omega) D_d$.

Note that $D_d^\dagger \hat{C}_x(\omega) D_d$ in $D_d^\dagger \hat{F}_{rp(x)}(\Omega) D_d$ is given by the quadrature $\hat{D}(\omega)$ and $\hat{A}(\omega)$ through Eq. (28). We consider the situation where the state for the input quadrature $\hat{A}(\omega)$ from the anti-symmetric port is vacuum and the state for the input quadrature $\hat{D}(\omega)$ from the symmetric port is the coherent state as Eq. (42) which enable us to separate the operator $\hat{D}(\omega)$ into the vacuum quadrature and the classical carrier as Eq. (46). Through Eqs. (28), (29) and (46), we may separate $D_d^\dagger \hat{C}_{x,y}(\omega) D_d$ into the vacuum quadrature and the classical carrier as

$$D_d^\dagger \hat{C}_{x,y}(\omega) D_d = \hat{C}_{x,y(c)}(\omega) + \hat{C}_{x,y(v)}(\omega), \quad (59)$$

where

$$\hat{C}_{x(c)}(\omega) = \hat{C}_{y(c)}(\omega) = \frac{1}{\sqrt{2}} \hat{D}_c(\omega), \quad (60)$$

$$\hat{C}_{x(v)}(\omega) := \frac{1}{\sqrt{2}} \left(\hat{D}_v(\omega) + \hat{A}(\omega) \right), \quad (61)$$

$$\hat{C}_{y(v)}(\omega) := \frac{1}{\sqrt{2}} \left(\hat{D}_v(\omega) - \hat{A}(\omega) \right). \quad (62)$$

Through Eqs. (55), (56), (59), (60), (61), and (62), and ignoring the

higher-order terms of the vacuum quadrature and displacement, we obtain

$$\begin{aligned}
& D_d^\dagger \hat{F}_{rp(x)}(\Omega) D_d \\
&= \frac{\hbar}{2c} e^{-i\theta/2} e^{+i\Omega\tau} \int \frac{d\omega}{2\pi} \sqrt{|\omega(\Omega - \omega)|} \left[\hat{D}_c(\omega) \hat{D}_c(\Omega - \omega) \right. \\
&\quad \left. + 2\hat{D}_c(\omega) \left(\hat{D}_v(\Omega - \omega) + \hat{A}(\Omega - \omega) \right) \right] \\
&\quad + i \frac{\hbar}{2c^2} e^{-i\theta/2} \iint \frac{d\omega}{2\pi} \frac{d\omega'}{2\pi} \sqrt{|\omega\omega'|} (\omega + \omega') \hat{D}_c(\omega) \hat{D}_c(\omega') \\
&\quad \times D_d^\dagger \hat{Z}_x(\Omega - \omega - \omega') D_d e^{+i(\omega+\omega')\tau}, \tag{63}
\end{aligned}$$

$$\begin{aligned}
& D_d^\dagger \hat{F}_{rp(y)}(\Omega) D_d \\
&= \frac{\hbar}{2c} e^{+i\theta/2} e^{+i\Omega\tau} \int \frac{d\omega}{2\pi} \sqrt{|\omega(\Omega - \omega)|} \left[\hat{D}_c(\omega) \hat{D}_c(\Omega - \omega) \right. \\
&\quad \left. + 2\hat{D}_c(\omega) \left(\hat{D}_v(\Omega - \omega) - \hat{A}(\Omega - \omega) \right) \right] \\
&\quad + i \frac{\hbar}{2c^2} e^{+i\theta/2} \iint \frac{d\omega}{2\pi} \frac{d\omega'}{2\pi} \sqrt{|\omega\omega'|} (\omega + \omega') \hat{D}_c(\omega) \hat{D}_c(\omega') \\
&\quad \times D_d^\dagger \hat{Z}_y(\Omega - \omega - \omega') D_d e^{+i(\omega+\omega')\tau}. \tag{64}
\end{aligned}$$

Through the expressions of the radiation-pressure forces (63) and (64), Eqs. (57) and (58) of the end-mirrors are given by

$$\begin{aligned}
& m\Omega^2 D_d^\dagger \hat{Z}_{com}(\Omega) D_d \\
&= -\frac{\hbar}{c} e^{+i\Omega\tau} \cos\left(\frac{\theta}{2}\right) \int \frac{d\omega}{2\pi} \sqrt{|\omega(\Omega - \omega)|} \hat{D}_c(\omega) \hat{D}_c(\Omega - \omega) \\
&\quad - \frac{2\hbar}{c} e^{+i\Omega\tau} \int \frac{d\omega}{2\pi} \sqrt{|\omega(\Omega - \omega)|} \hat{D}_c(\omega) \left(\cos\left(\frac{\theta}{2}\right) \hat{D}_v(\Omega - \omega) \right. \\
&\quad \quad \left. - i \sin\left(\frac{\theta}{2}\right) \hat{A}(\Omega - \omega) \right) \\
&\quad - i \cos\left(\frac{\theta}{2}\right) \frac{\hbar}{c^2} \iint \frac{d\omega}{2\pi} \frac{d\omega'}{2\pi} \sqrt{|\omega\omega'|} (\omega + \omega') \hat{D}_c(\omega) \hat{D}_c(\omega') \\
&\quad \quad \times D_d^\dagger \hat{Z}_{com}(\Omega - \omega - \omega') D_d e^{+i(\omega+\omega')\tau} \\
&\quad - \sin\left(\frac{\theta}{2}\right) \frac{\hbar}{c^2} \iint \frac{d\omega}{2\pi} \frac{d\omega'}{2\pi} \sqrt{|\omega\omega'|} (\omega + \omega') \hat{D}_c(\omega) \hat{D}_c(\omega') \\
&\quad \quad \times D_d^\dagger \hat{Z}_{diff}(\Omega - \omega - \omega') D_d e^{+i(\omega+\omega')\tau}, \tag{65}
\end{aligned}$$

$$\begin{aligned}
& m\Omega^2 D_d^\dagger \hat{Z}_{diff}(\Omega) D_d \\
&= i \sin\left(\frac{\theta}{2}\right) \frac{\hbar}{c} e^{+i\Omega\tau} \int \frac{d\omega}{2\pi} \sqrt{|\omega(\Omega - \omega)|} \hat{D}_c(\omega) \hat{D}_c(\Omega - \omega) \\
&\quad + \frac{2\hbar}{c} e^{+i\Omega\tau} \int \frac{d\omega}{2\pi} \sqrt{|\omega(\Omega - \omega)|} \hat{D}_c(\omega) \left(i \sin\left(\frac{\theta}{2}\right) e^{+i\theta/2} \hat{D}_v(\Omega - \omega) \right. \\
&\qquad\qquad\qquad \left. - \cos\left(\frac{\theta}{2}\right) \hat{A}(\Omega - \omega) \right) \\
&\quad - \sin\left(\frac{\theta}{2}\right) \frac{\hbar}{c^2} \iint \frac{d\omega}{2\pi} \frac{d\omega'}{2\pi} \sqrt{|\omega\omega'|} (\omega + \omega') \hat{D}_c(\omega) \hat{D}_c(\omega') \\
&\qquad\qquad\qquad \times D_d^\dagger \hat{Z}_{com}(\Omega - \omega - \omega') D_d e^{+i(\omega + \omega')\tau} \\
&\quad - i \cos\left(\frac{\theta}{2}\right) \frac{\hbar}{c^2} \iint \frac{d\omega}{2\pi} \frac{d\omega'}{2\pi} \sqrt{|\omega\omega'|} (\omega + \omega') \hat{D}_c(\omega) \hat{D}_c(\omega') \\
&\qquad\qquad\qquad \times D_d^\dagger \hat{Z}_{diff}(\Omega - \omega - \omega') D_d e^{+i(\omega + \omega')\tau} \\
&\quad + \frac{1}{2} m L \Omega^2 h(\Omega). \tag{66}
\end{aligned}$$

The explicit representations of $D_d^\dagger \hat{Z}_{com}(\Omega) D_d$ and $D_d^\dagger \hat{Z}_{diff}(\Omega) D_d$ are given as the solutions to Eqs. (65) and (66), respectively. Through these solutions, we can evaluate the input-output relation (49) in a closed form.

3.3. Remarks

Here, we describe some remarks on the results of this section.

In Eq. (49), we extend the state of the photon field from the light source from the monochromatic laser, which is described by the δ -function complex amplitude for the coherent state whose support only at the $\omega = \omega_0$, to an arbitrary coherent state whose complex amplitude is described by an arbitrary function $\alpha(\omega)$ in the frequency domain. Due to this extension, in Eq. (49), we have to evaluate the convolution in the frequency domain, while the integration for this convolution is simplified due to the δ -function in the conventional Michelson gravitational-wave detectors. Since the complex amplitude for the coherent state from the light source is arbitrary in Eq. (49), we do not have central frequency ω_0 of the complex amplitude, the sideband picture around this central frequency, nor the approximation $\omega_0 \gg \Omega$. These are due to the fact that we did not use the two-photon formulation.

Furthermore, we introduce the phase offset θ in the input-output relation (49). Due to this phase offset θ , Eq. (49) has some effects which are not

taken into account in the input-output relation for the conventional Michelson gravitational-wave detector. The first one is the leakage of the classical carrier field from the light source and the second one is the shot noise from the light source. These are described by the first and second terms in the right-hand side of Eq. (49), respectively. The final one is the effect of common motion of the two end-mirrors, which is described by the second line in Eq. (49). This common motion $D_d^\dagger \hat{Z}_{com}(\Omega) D_d$ together with the differential motion $D_d^\dagger \hat{Z}_{diff}(\Omega) D_d$ in Eq. (49) is determined by the equations of motion of two end-mirrors which are given by Eqs. (65) and (66).

The equations of motion (65) and (66) are also modified due to our extension. For example, in the equation (66) for the differential motion of the end-mirrors, we have to evaluate the convolution in the first four lines in the right-hand side due to the extension of the complex amplitude for the coherent state from the δ -function $\delta(\omega - \omega_0)$ to an arbitrary function $\alpha(\omega)$ in the frequency domain. Furthermore, the third and fourth lines in the right-hand side of Eq. (66) appear due to this extension. These terms do not appear in the equations of motion for the end-mirrors in the conventional Michelson gravitational-wave detector, and arise due to the modulation of the shape of the complex amplitude by the retarded effect due to the optical field propagation from the central beam splitter to the end-mirrors. Moreover, the direct effect due to the classical carrier part from the light sources and the effect due to the shot noise from the light source appears which affects the differential motion of end-mirrors through the introduction of the phase offset θ .

Thus, we regard that the set of the input-output relation for the extended Michelson interferometer (49), equations (65) and (66) of motions for the end-mirrors is the main result of this paper.

4. Re-derivation of conventional input-output relation

In this section, we show that the derived input-output relation (49) with equations (65) and (66) of motions yields the input-output relation for the conventional Michelson interferometric gravitational-wave detector.

4.1. Input-output relation

In the conventional Michelson gravitational-wave detector, the state of the optical beam from the light source is in the coherent state with the complex amplitude

$$\alpha(\omega) = 2\pi N \delta(\omega - \omega_0). \quad (67)$$

We note that $\alpha(\omega)$ is real. The corresponding electric field with the amplitude (67) of $\alpha(\omega)$ is the continuous monochromatic carrier field with the frequency ω_0 . The normalization factor N is related to the averaged photon number per second

$$N = \sqrt{\frac{I_0}{\hbar\omega_0}}, \quad (68)$$

where I_0 is the averaged power of the carrier field. Through the definition (47), the classical part $\hat{D}_c(\omega)$ of the input light source is given by

$$\hat{D}_c(\omega) = 2\pi N \{ \delta(\omega - \omega_0)\Theta(\omega) + \delta(\omega + \omega_0)\Theta(-\omega) \}. \quad (69)$$

Here, we concentrate on the mode with the frequency $\omega_0 \pm \Omega$. For these sidebands, $\hat{D}_c(\omega)$ given by Eq. (69) includes terms which depend on $2\omega_0 \pm \Omega$. In the time-domain, these terms includes the factor of the rapid oscillation $e^{i2\omega_0 t}$. Therefore, this part can be removed in the data taking or the data analyses processes and we ignore these terms, since we concentrate only on the fluctuations with the frequency $\omega_0 \pm \Omega$. For this reason, $\hat{D}_c(\omega)$ with $\omega_0 \pm \Omega$ may be regarded as

$$\hat{D}_c(\omega_0 \pm \Omega) = 2\pi N \delta(\Omega). \quad (70)$$

Through the same approximation, the input-output relations (49) with $\omega = \omega_0 \pm \Omega$ are given by

$$\begin{aligned} & e^{-2i(\omega_0 \pm \Omega)\tau} D_d^\dagger \hat{B}(\omega_0 \pm \Omega) D_d \\ &= i \sin\left(\frac{\theta}{2}\right) \hat{D}_c(\omega_0 \pm \Omega) + i \sin\left(\frac{\theta}{2}\right) \hat{D}_v(\omega_0 \pm \Omega) + \cos\left(\frac{\theta}{2}\right) \hat{A}(\omega_0 \pm \Omega) \\ & \quad + \frac{2iN\omega_0^{3/2} e^{\mp i\Omega\tau}}{c\sqrt{|\omega_0 \pm \Omega|}} \left[i \sin\left(\frac{\theta}{2}\right) D_d^\dagger \hat{Z}_{com}(\pm\Omega) D_d \right. \\ & \quad \left. - \cos\left(\frac{\theta}{2}\right) D_d^\dagger \hat{Z}_{diff}(\pm\Omega) D_d \right], \end{aligned} \quad (71)$$

and Eqs. (65) and (66) are given by

$$\begin{aligned}
& m\Omega^2 D_d^\dagger \hat{Z}_{com}(\Omega) D_d \\
&= -\frac{\hbar N e^{+i\Omega\tau} \sqrt{\omega_0}}{c} \cos\left(\frac{\theta}{2}\right) \left(\sqrt{|\Omega - \omega_0|} \hat{D}_c(\Omega - \omega_0) \right. \\
&\quad \left. + \sqrt{|\Omega + \omega_0|} \hat{D}_c(\Omega + \omega_0) \right) \\
&\quad - \frac{2\hbar N e^{+i\Omega\tau} \sqrt{\omega_0}}{c} \left\{ \sqrt{|\Omega - \omega_0|} \left(\cos\left(\frac{\theta}{2}\right) \hat{D}_v(\Omega - \omega_0) \right. \right. \\
&\quad \left. \left. - i \sin\left(\frac{\theta}{2}\right) \hat{A}(\Omega - \omega_0) \right) \right. \\
&\quad \left. + \sqrt{|\Omega + \omega_0|} \left(\cos\left(\frac{\theta}{2}\right) \hat{D}_v(\Omega + \omega_0) \right. \right. \\
&\quad \left. \left. - i \sin\left(\frac{\theta}{2}\right) \hat{A}(\Omega + \omega_0) \right) \right\}, \quad (72)
\end{aligned}$$

$$\begin{aligned}
& m\Omega^2 D_d^\dagger \hat{Z}_{diff}(\Omega) D_d \\
&= +\frac{i\hbar N e^{+i\Omega\tau} \sqrt{\omega_0}}{c} \sin\left(\frac{\theta}{2}\right) \left\{ \sqrt{|\Omega - \omega_0|} \hat{D}_c(\Omega - \omega_0) \right. \\
&\quad \left. + \sqrt{|\Omega + \omega_0|} \hat{D}_c(\Omega + \omega_0) \right\} \\
&\quad + \frac{2\hbar N e^{+i\Omega\tau} \sqrt{\omega_0}}{c} \left\{ \sqrt{|\Omega - \omega_0|} \left[i \sin\left(\frac{\theta}{2}\right) \hat{D}_v(\Omega - \omega_0) \right. \right. \\
&\quad \left. \left. - \cos\left(\frac{\theta}{2}\right) \hat{A}(\Omega - \omega_0) \right] \right. \\
&\quad \left. + \sqrt{|\Omega + \omega_0|} \left[i \sin\left(\frac{\theta}{2}\right) \hat{D}_v(\Omega + \omega_0) \right. \right. \\
&\quad \left. \left. - \cos\left(\frac{\theta}{2}\right) \hat{A}(\Omega + \omega_0) \right] \right\} \\
&\quad + \frac{1}{2} m L \Omega^2 h(\Omega). \quad (73)
\end{aligned}$$

Here, we consider the situation where $\omega_0 \gg \Omega$ and we apply the approximation in which $\omega_0 \pm \Omega$ in the coefficients of the input-output relation are regarded as $\omega_0 \pm \Omega \sim \omega_0$. Furthermore, we use

$$\omega_0 \tau = \omega_0 \frac{L}{c} = 2n\pi, \quad n \in \mathbb{N}, \quad (74)$$

so that the anti-symmetric port is the dark port. We also introduce the following variables

$$\kappa := \frac{8\omega_0 I_0}{mc^2 \Omega^2}, \quad h_{SQL} := \sqrt{\frac{8\hbar}{m\Omega^2 L^2}}. \quad (75)$$

In addition, since $\omega_0 \gg \Omega$, we should regard $\omega_0 + \Omega > 0$ and $\Omega - \omega_0 < 0$. Then, the substitution of Eqs. (72) and (73) into Eq. (71) yields the input-output relations as

$$\begin{aligned} D_d^\dagger \hat{b}_\pm D_d &= \sin\left(\frac{\theta}{2}\right) \left(i + \kappa \cos\left(\frac{\theta}{2}\right) \right) \sqrt{\frac{I_0}{\hbar\omega_0}} 2\pi\delta(\Omega) \\ &+ e^{\pm 2i\Omega\tau} \left[i \sin\left(\frac{\theta}{2}\right) \hat{d}_\pm + \cos\left(\frac{\theta}{2}\right) \hat{a}_\pm \right] \\ &+ \frac{\kappa e^{\pm 2i\Omega\tau}}{2} \left[\sin\theta \left(\hat{d}_\mp^\dagger + \hat{d}_\pm \right) \right. \\ &\quad \left. + i \cos\theta \left(\hat{a}_\mp^\dagger + \hat{a}_\pm \right) \right] \\ &- i\sqrt{\kappa} e^{\pm i\Omega\tau} \cos\left(\frac{\theta}{2}\right) \frac{h(\pm\Omega)}{h_{SQL}}, \end{aligned} \quad (76)$$

where $\hat{a}_\pm := \hat{a}(\omega_0 \pm \Omega)$, $\hat{b}_\pm := \hat{b}(\omega_0 \pm \Omega)$, and $\hat{d}_\pm := \hat{d}(\omega_0 \pm \Omega)$. Here, we note that the carrier part in Eq. (76), which is proportional to $\delta(\Omega)$ diverges due to the radiation-pressure contribution $\kappa \propto \Omega^{-2}$. Since we can predict this divergent part and can be removed by the data taking or the data analysis processes, this carrier part is ignored.

4.2. Two-photon formulation

Here, we note that the two-photon formulation is applicable in our situation $\omega_0 \gg \Omega$ and we introduce the operators

$$\hat{a}_1 = \frac{1}{\sqrt{2}}(\hat{a}_+ + \hat{a}_-^\dagger), \quad \hat{a}_2 = \frac{1}{\sqrt{2}i}(\hat{a}_+ - \hat{a}_-^\dagger), \quad (77)$$

$$\hat{b}_1 = \frac{1}{\sqrt{2}}(\hat{b}_+ + \hat{b}_-^\dagger), \quad \hat{b}_2 = \frac{1}{\sqrt{2}i}(\hat{b}_+ - \hat{b}_-^\dagger), \quad (78)$$

$$\hat{d}_1 = \frac{1}{\sqrt{2}}(\hat{d}_+ + \hat{d}_-^\dagger), \quad \hat{d}_2 = \frac{1}{\sqrt{2}i}(\hat{d}_+ - \hat{d}_-^\dagger). \quad (79)$$

In the two-photon formulation which treats the situation where the carrier field is proportional to $\cos\omega_0 t$, \hat{a}_1 , \hat{b}_1 , and \hat{d}_1 are regarded as amplitude

quadratures. On the other hand, \hat{a}_2 , \hat{b}_2 , and \hat{d}_2 are regarded as phase quadratures. Through these amplitude and phase quadratures, the input-output relation (76) yields

$$\begin{aligned}
D_d^\dagger \hat{b}_1 D_d &= \frac{1}{\sqrt{2}} \sin \theta \kappa \sqrt{\frac{I_0}{\hbar \omega_0}} 2\pi \delta(\Omega) \\
&+ e^{+2i\Omega\tau} \left\{ -\sin\left(\frac{\theta}{2}\right) \hat{d}_2 + \cos\left(\frac{\theta}{2}\right) \hat{a}_1 \right\} \\
&+ e^{+2i\Omega\tau} \kappa \sin \theta \hat{d}_1,
\end{aligned} \tag{80}$$

$$\begin{aligned}
D_d^\dagger \hat{b}_2 D_d &= \sqrt{2} \sin\left(\frac{\theta}{2}\right) \sqrt{\frac{I_0}{\hbar \omega_0}} 2\pi \delta(\Omega) \\
&+ e^{+2i\Omega\tau} \left\{ \sin\left(\frac{\theta}{2}\right) \hat{d}_1 + \cos\left(\frac{\theta}{2}\right) \hat{a}_2 \right\} \\
&+ \cos \theta e^{+2i\Omega\tau} \kappa \hat{a}_1 \\
&- e^{+i\Omega\tau} \cos\left(\frac{\theta}{2}\right) \sqrt{2\kappa} \frac{h(\Omega)}{h_{SQL}}.
\end{aligned} \tag{81}$$

In Eq. (80), the first term is the divergent classical carrier field induced by the radiation pressure force due to the mirror motion. The second term is the shot noise from the quantum fluctuations from the bright port and the dark port. The last term in Eq. (80) is the radiation pressure noise due to the mirror motion which originally comes from the quantum fluctuation in the incident optical beam from the bright port. On the other hand, in Eq. (81), the first term is the classical carrier field which leaks from the light source by the phase offset θ . The second term is the shot noise from the quantum fluctuation from the bright port and the dark port. The third line is the radiation pressure noise due to the mirror motion which originally comes from the quantum fluctuations in the vacuum from the dark port. The last term is the gravitational-wave signal.

Although the classical carrier parts in $D_d^\dagger \hat{b}_1 D_d$ and $D_d^\dagger \hat{b}_2 D_d$ is completely determined in classical sense and can be removed in the data analysis, we also note that the classical carrier part which diverge due to the radiation pressure force contributes only to the amplitude quadrature $D_d^\dagger \hat{b}_1 D_d$. Therefore, as far as we observe only $D_d^\dagger \hat{b}_2 D_d$ [14], the divergent term due to the radiation pressure force cancels and we do not have to care about this divergence.

Finally, we note that if we choose $\theta = 0$, Eqs. (80) and (81) are reduced

to

$$D_d^\dagger \hat{b}_1 D_d = e^{+2i\Omega\tau} \hat{a}_1, \quad (82)$$

$$D_d^\dagger \hat{b}_2 D_d = e^{+2i\Omega\tau} (\hat{a}_2 + \kappa \hat{a}_1) - e^{+i\Omega\tau} \sqrt{2\kappa} \frac{h(\Omega)}{h_{SQL}}, \quad (83)$$

respectively. This is the conventional input-output relation for the Michelson gravitational-wave detector [13]. This means that the input-output relation (80) and (81) are recover the usual input-output relation which is well-known in the gravitational-wave community. Furthermore, this also means that the set of the original input-output relation (49) and Eqs. (65) and (66) of mirrors' motions are the natural extension of the conventional input-output relation of the Michelson interferometric gravitational-wave detector.

5. Weak-value amplification from the extended input-output relation

Here, we consider the situation of the weak measurement in the interferometer setup depicted in Fig. 1 from the input-output relation (49) to show that this input-output relation actually includes the weak-value amplification. Without loss of generality, we may choose $\omega > 0$ in Eq. (49):

$$\begin{aligned} & e^{-2i\omega\tau} D_d^\dagger \hat{b}(\omega) D_d \\ &= i \sin\left(\frac{\theta}{2}\right) \alpha(\omega) + i \sin\left(\frac{\theta}{2}\right) \hat{d}(\omega) + \cos\left(\frac{\theta}{2}\right) \hat{a}(\omega) \\ & \quad + \frac{2i}{c} \int_{-\infty}^{+\infty} \frac{d\Omega}{2\pi} e^{-i\Omega\tau} \sqrt{\left|\frac{\omega - \Omega}{\omega}\right|} (\omega - \Omega) \\ & \quad \times \left[i \sin\left(\frac{\theta}{2}\right) \hat{D}_c(\omega - \Omega) D_d^\dagger \hat{Z}_{com}(\Omega) D_d \right. \\ & \quad \left. - \cos\left(\frac{\theta}{2}\right) \hat{D}_c(\omega - \Omega) D_d^\dagger \hat{Z}_{diff}(\Omega) D_d \right]. \quad (84) \end{aligned}$$

To discuss the weak measurement from this input-output relation, we concentrate on the output photon number operator $\hat{n}(\omega)$ to the photo-detector

$$\hat{n}(\omega) := \hat{b}^\dagger(\omega) \hat{b}(\omega) \quad (85)$$

and its expectation value in the state (42) is given by

$$\begin{aligned}\overline{n(\omega)} &:= \langle \psi | \hat{n}(\omega) | \psi \rangle \\ &= \langle 0|_a \otimes \langle 0|_d \left(D_d^\dagger \hat{b}(\omega) D_d \right)^\dagger \left(D_d^\dagger \hat{b}(\omega) D_d \right) | 0 \rangle_a \otimes | 0 \rangle_d\end{aligned}\quad (86)$$

Here, we consider the situation where \hat{Z}_{com} and \hat{Z}_{diff} are classical, i.e., proportional to the identity operator in the sense of quantum theory and their frequency-dependence are negligible. Furthermore, the complex amplitude $\alpha(\omega)$ for the coherent state from the light source is real and has its compact support within the frequency $\omega \in [0, \infty]$ and is rapidly decreasing at the boundaries $\omega \rightarrow 0$ and $\omega \rightarrow +\infty$ of this range. This is the situation discussed by Nishizawa in Ref. [7].

Substituting Eq. (84) into Eq. (86), and taking the linear term with respect to \hat{Z}_{com} and \hat{Z}_{diff} , we obtain

$$\begin{aligned}\overline{n(\omega)} &= \sin^2\left(\frac{\theta}{2}\right) \alpha^2(\omega) \\ &\quad - \sin^2\left(\frac{\theta}{2}\right) \frac{8}{2\pi c \omega^{1/2}} \mathcal{I}_{s+3/2}(\tau, \alpha) \alpha(\omega) \\ &\quad \times \left(\cos(\omega\tau) \hat{Z}_{com} + \cot\left(\frac{\theta}{2}\right) \sin(\omega\tau) \hat{Z}_{diff} \right),\end{aligned}\quad (87)$$

where we introduce the definite integral $\mathcal{I}_{s+3/2}(\tau, \alpha)$ defined by

$$\mathcal{I}_{s+3/2}(\tau, \alpha) := \int_0^{+\infty} dx x^{3/2} \sin(x\tau) \alpha(x). \quad (88)$$

When $\alpha(\omega)$ is given by the Gaussian function, this definite integral $\mathcal{I}_{s+3/2}(\tau, \alpha)$ does converge and expressed using the parabolic cylinder function [16]. Here, we define $\overline{n_0(\omega)}$ and $\delta n(\omega)$ by

$$\overline{n_0(\omega)} := \sin^2\left(\frac{\theta}{2}\right) \alpha^2(\omega), \quad (89)$$

$$\begin{aligned}\delta n(\omega) &:= -\sin^2\left(\frac{\theta}{2}\right) \frac{8}{2\pi c \sqrt{\omega}} \mathcal{I}_{s+3/2}(\tau, \alpha) \alpha(\omega) \\ &\quad \times \left(\cos(\omega\tau) \hat{Z}_{com} + \cot\left(\frac{\theta}{2}\right) \sin(\omega\tau) \hat{Z}_{diff} \right),\end{aligned}\quad (90)$$

so that

$$\overline{n(\omega)} = \overline{n_0(\omega)} + \delta n(\omega). \quad (91)$$

As explained in Sec. 2.2, we consider the normalized frequency distribution $f(\omega)$ of the output photon number defined by Eq. (11). We evaluate the expectation value of the frequency ω under the distribution function $f(\omega)$ as

$$\begin{aligned} \langle \omega \rangle &:= \int_0^{+\infty} d\omega \omega f(\omega) \\ &\sim \omega_0 + \frac{\int_0^{+\infty} d\omega (\omega - \omega_0) \delta n(\omega)}{\int_0^{+\infty} d\omega \overline{n_0(\omega)}}, \end{aligned} \quad (92)$$

where we denoted

$$\omega_0 := \frac{\int_0^{+\infty} d\omega \omega \overline{n_0(\omega)}}{\int_0^{+\infty} d\omega \overline{n_0(\omega)}}. \quad (93)$$

Furthermore, we introduce following definite integrals

$$\mathcal{J}(\alpha) := \int_0^{+\infty} d\omega \alpha^2(\omega), \quad (94)$$

$$\mathcal{I}_{c\pm 1/2}(\tau, \alpha) := \int_0^{+\infty} dx x^{\pm 1/2} \cos(x\tau) \alpha(x), \quad (95)$$

$$\mathcal{I}_{s\pm 1/2}(\tau, \alpha) := \int_0^{+\infty} dx x^{\pm 1/2} \sin(x\tau) \alpha(x). \quad (96)$$

When $\alpha(\omega)$ is the Gaussian function, these definite integrals do converge. Using these definite integrals, the expectation value (92) of the frequency ω under the distribution function (11) is given by

$$\begin{aligned} \langle \omega \rangle - \omega_0 &\sim \hat{Z}_{com} \frac{8}{2\pi c \mathcal{J}(\alpha)} \mathcal{I}_{s+3/2}(\tau, \alpha) \\ &\quad \times (\omega_0 \mathcal{I}_{c-1/2}(\tau, \alpha) - \mathcal{I}_{c+1/2}(\tau, \alpha)) \\ &+ \cot\left(\frac{\theta}{2}\right) \hat{Z}_{diff} \frac{8}{2\pi c \mathcal{J}(\alpha)} \mathcal{I}_{s+3/2}(\tau, \alpha) \\ &\quad \times (\omega_0 \mathcal{I}_{s-1/2}(\tau, \alpha) - \mathcal{I}_{s+1/2}(\tau, \alpha)). \end{aligned} \quad (97)$$

When $\theta \ll 1$, the second term in Eq. (97) is dominant, i.e.,

$$\begin{aligned} \langle \omega \rangle - \omega_0 \sim & +\frac{2}{\theta} \hat{Z}_{diff} \frac{8}{2\pi c \mathcal{J}(\alpha)} \mathcal{I}_{s+3/2}(\tau, \alpha) \\ & \times (\omega_0 \mathcal{I}_{s-1/2}(\tau, \alpha) - \mathcal{I}_{s+1/2}(\tau, \alpha)). \end{aligned} \quad (98)$$

This is the weak-value amplification effect.

We note that there is no effect of the quantum fluctuations which described by the quadratures \hat{a} nor \hat{d} , but completely determined by the amplitude $\alpha(\omega)$ of the coherent state for the quadrature \hat{d} . We also note that these arguments does not seriously depend on the details of the real function $\alpha(\omega)$.

Thus, we have shown that our derived input-output relation (49) actually includes the situation of the weak-value amplification.

6. Summary and discussion

In this paper, we considered the extension of the input-output relation for a conventional Michelson gravitational-wave detector to compare the weak-measurement inspired gravitational-wave detector in Ref. [7] with conventional one. The main difference between these detectors is the injected optical field, which is a continuous monochromatic laser in conventional one and is the continuous pulse beam in the model of Ref. [7]. Therefore, we extend the conventional input-output relation for the gravitational-wave detector to the situation where the injected photon state is a coherent state with an arbitrary complex amplitude $\alpha(\omega)$. We also showed that our extended input-output relation actually includes both situations of conventional gravitational-wave detectors and that where the weak-value amplification occurs. This is the main result of this paper.

Within this paper, we do not discuss quantum noise in the situation where the weak-value amplification occurs. However, in principle, we will be able to discuss quantum noises, i.e., the shot noise and the radiation-pressure noise due to the quantum fluctuations of photons in the Michelson interferometric gravitational-wave detector, even in the situation where the weak-value amplification occurs. In our derivation, we regard that the Fourier transformed variables describes the situation of the stationary continuous measurement through the average of the many pulses. Although this stationarity is an

assumption throughout this paper, we can discuss the time-evolution of the gravitational-wave signal through the frequency dependence of the mirror displacement in the extended input-output relation in Sec. 3. This is the difference from discussions in Ref. [7] which assume that the mirror displacement is constant in time. In Sec. 5, we just dare to consider the situation where the mirror displacement is constant in time just for the comparison with Ref. [7]. For this reason, we should regard that our derived input-output relation in Sec. 3 is different from that derived in Ref. [7].

In spite of this difference from Ref. [7], we reached to the same conclusions as those in Ref. [7]. First, as discussed in Sec. 5, the weak-value amplification from the input-output relation (49) is the effect due to the carrier field $\alpha(\omega)$ of the coherent state from the light source and has nothing to do with the quantum fluctuations described by the annihilation and creation operators for photon. Second, together with the amplification of the gravitational-wave signal, the weak-value amplification also amplifies the radiation-pressure noise which is one of important quantum noise in gravitational-wave detectors. These two conclusions are not affected by the details of the analyses. In this sense, these are robust. In addition to the above two conclusions, from the comparison between the input-output relations (76) in Sec. 4 and Eq. (84) in Sec. 5, we may say that a conventional Michelson gravitational-wave detector already includes the essence of the weak-value amplification as the reduction of the quantum noise from the light source through the measurement at the dark port as the final conclusion.

In the situation where the weak-value amplification occurs discussed in Sec. 5, the unperturbed photon number, i.e., the first term in the right-hand side of Eq. (87), proportional to $\sin^2(\theta/2)$ and there are factors $\sin^2(\theta/2)$ and $\sin(\theta/2)\cos(\theta/2)$ in the coefficients of \hat{Z}_{com} and \hat{Z}_{diff} , respectively. Since we consider the expectation value of ω under the conditional photon-number distribution $f(\omega)$ defined by Eq. (11), we divide the perturbed terms, i.e., the second term in the right-hand side of Eq. (87) which are proportional to \hat{Z}_{com} or \hat{Z}_{diff} , by the unperturbed photon number in Eq. (87). Through this process, the factor $\sin^2(\theta/2)$ in the coefficient of the term including \hat{Z}_{com} canceled out, but the coefficient of the \hat{Z}_{diff} becomes $\cot(\theta/2)$. Then, if we choose $\theta \ll 1$, the term which includes \hat{Z}_{diff} is dominant. This is the weak-value amplification. Actually, the weak value in our setup depicted in Fig. 1 is proportional to $\cot(\theta/2)$ as shown in Eq. 6. The important point is the fact that the weak-value amplifies \hat{Z}_{diff} which includes not only gravitational-

wave signal $h(\Omega)$ but also the radiation-pressure noise. Therefore, we cannot improve the signal to noise ratio by the weak-value amplification at least in the simple model in this paper as pointed out by Nishizawa [7]. Since the reduction of these noises from the dark-port is the main target in some researches of gravitational-wave detectors, this model is not useful for this target.

On the other hand, we compare of input-output relations (76) and (84) through the original input-output relation (71). The coefficients of \hat{Z}_{com} and \hat{Z}_{diff} in Eq. (97), which yields the weak-value amplification, are determined by the last term in the input-output relation Eq. (84). The same $(\sin(\theta/2), \cos(\theta/2))$ -dependence in the input-output relation can be seen in the original input-output relation (49). The same dependence can also be seen in the input-output relation (71) for the conventional gravitational-wave detector and subsequent input-output relations (76), (80) and (81). Therefore, the same effect as the weak-value amplification is already included in the conventional Michelson-interferometric gravitational-wave detector through the photon detection at the anti-symmetric port which are nearly dark-port. We may say that the common motion \hat{Z}_{com} and, equivalently, the quantum fluctuations associated with the quadrature \hat{d} which affect the input-output relation through \hat{Z}_{com} are negligible due to the the weak-value amplification. This is the meaning of the above final conclusion.

Although the model discussed here is not useful for the reduction of the quantum noise at the dark port in a gravitational-wave detector, there are still rooms to discuss the weak-measurement inspired gravitational-wave detector. One of the issues to be clarified is the effect due to the optical pulse injection from the light source instead of the monochromatic continuous optical laser in the conventional gravitational-wave detectors. As the first step of this research is to examination of the input-output relation of (49) without the approximation in which we regard that \hat{Z}_{com} and \hat{Z}_{diff} are almost constant, while our arguments in Sec. 5 are based on this approximation. This examination will leads to discussion of the direct comparison with the conventional Michelson-interferometric gravitational-wave detector. To complete this discussion, we have to examine the problem whether or not the assumptions which are introduced when we derive the conventional input-output relations (82) and (83) are also valid even in the model of Ref. [7]. First, to derive these input-output relations, we concentrate on the sidebands $\omega_0 \pm \Omega$ as Eq. (71). We have to discuss the sideband picture is appropriate for the weak-measurement or not. As far as the discussion within the level

of Sec. 5 in this paper, we cannot apply the sideband-picture in the weak-measurement inspired gravitational-wave detector. Second, in the derivation of Eq. (82) and (83), we ignored the high frequency modes with the frequency $2\omega_0 \pm \Omega$. On the other hand, in our weak measurement model, we consider the broad frequency distribution of the photon field in Sec. 5. We have to judge whether we can ignore the high frequency modes even in the weak-measurement inspired gravitational-wave detector, or not. Finally, we considered the situation $\omega_0 \gg \Omega$ in the derivation of Eq. (82) and (83). This will not be appropriate in the weak-measurement inspired gravitational-wave detector.

In addition to the above problem, the input-output relation (49) might not converge due to the response of the detector. This will be the most important issue for the model in Ref. [7]. Roughly speaking, $D_d^\dagger \hat{Z}_{com}(\Omega) \hat{D}_d$ and $D_d^\dagger \hat{Z}_{diff}(\Omega) \hat{D}_d$ will have the pole proportional to $1/\Omega^2$ through the equations of motion (65) and (66). If $\hat{D}_c(\omega - \Omega)$ in Eq. (49) basically given by the Gaussian function, the integrand in Eq. (49) might diverge due to this pole $1/\Omega^2$. If this divergence is true and important in our situation, we have to carefully discuss the physical meaning of this divergence and treat it delicately.

We have to carefully discuss these issues for the complete comparison between the weak-measurement inspired gravitational-wave detector and the conventional Michelson gravitational-wave detector. However, these issues are beyond the current scope of this paper. Therefore, we leave this comparison with conventional gravitational-wave detectors as one of future works.

Even if we complete the arguments in the case where \hat{Z}_{com} and \hat{Z}_{diff} are not constant, we might reach to the conclusion that the conventional Michelson-interferometric gravitational-wave detector is more appropriate as a gravitational-wave detector than weak-measurement inspired gravitational-wave detectors. However, even in this case, we will be able to discuss the effect of the pulse-train light source. In the experimental optics, there is a report on the ultrashort optical pulse trains produced by the mode lock laser, which states that there are shot noise correlations in the frequency domain of an ultrashort optical pulse trains and we can reduce the shot noise using this correlation [17]. If we can use the same technique as this experiment, there is a possibility to reduce the shot noise through the correlations in the ultrashort optical pulse train produced by the mode-lock laser. Of-course, this is no longer the weak-value amplification but this idea comes from the point of view inspired by the weak measurements. We will hope that our discussion

in this paper will be useful when we discuss this interesting possibility. We also leave this interesting possibility as one of future works.

Acknowledgments

K.N. acknowledges to Dr. Tomotada Akutsu and the other members of the gravitational-wave project office in NAOJ for their continuous encouragement to our research. K.N. also appreciate Prof. Akio Hosoya and Prof. Izumi Tsutsui for their support and continuous encouragement.

References

- [1] Y. Aharonov, D. Z. Albert, and L. Vaidman, Phys. Rev. Lett. **60** (1988), 1351.
- [2] N. W. M. Ritchie, J. G. Story, and R. G. Hulet, Phys. Rev. Lett. **66** (1991), 1107. O. Hosten and P. Kwiat, Science **319** (2008), 787; K.J.Resch, Science **319** (2008), 733. P. B. Dixon, D. J. Starling, A. N. Jordan, and J. C. Howell, Phys. Rev. Lett. **102** (2009), 173601; D. J. Starling, P. B. Dixon, A. N. Jordan, and J. C. Howell, Phys. Rev. A **80** (2009), 041803(R); D. J. Starling, P. B. Dixon, A. N. Jordan, and J. C. Howell, Phys. Rev. A **82** (2010), 063822; D. J. Starling, P. B. Dixon, N. S. Williams, A. N. Jordan, and J. C. Howell, Phys. Rev. A **82** (2010), 011802(R). M. Iinuma, Y. Suzuki, G. Taguchi, Y. Kadoya, and H. F. Hofmann, New J. Phys. **13** (2011), 033041. G. I. Viza, J. Martínez-Rincón, G. A. Howland, H. Frostig, I. Shomroni, B. Dayan, and J. C. Howell, Optics Letters **38** (2013), 2949.
- [3] B. P. Abbot et al., Phys. Rev. Lett. **116** (2016), 061102; *ibid.* **116** (2016), 241103.
- [4] K. Nakamura, A. Nishizawa, and Masa-Katsu Fujimoto, Phys. Rev. A **85** (2012), 012113.
- [5] A. Nishizawa, K. Nakamura, and Masa-Katsu Fujimoto, Phys. Rev. A **85** (2012), 062108.
- [6] K. Nakamura, M. Iinuma, Phys. Rev. A **88** (2013), 042106.
- [7] A. Nishizawa, Phys. Rev. A **92** (2015), 032123.

- [8] C. M. Caves, and B. L. Schumaker, Phys. Rev. A **31** (1985), 3068; *ibid.* **31** (1985), 3093.
- [9] C. W. Misner, T. S. Thorne, and J. A. Wheeler, *Gravitation* (Freeman, San Francisco, 1973)
- [10] In the actual gravitational-wave detectors, the similar phase offset is introduced in the different context. When the arm length L is chosen so that the anti-symmetric port is completely dark port, the response of the interferometer to gravitational-wave propagation is maximum. However, in this maximum response, we cannot measure the phase of gravitational wave due to the symmetry of the interferometer. Since detected photon numbers are continuously monitored and the feedback-control technique is used so that the anti-symmetric port is always almost dark port with this finite phase offset. This feedback-control electric current is the actual data of the gravitational-wave observation. At the complete dark port, this feedback-control technique is not applicable.
- [11] H. J. Kimble, Y. Levin, A. B. Matsko, K. S. Thorne, and S. P. Vyatchanin, Phys. Rev. D **65** (2001), 022002.
- [12] In quantum mechanics, Eqs. (21), (26), and (27) are described by the unitary transformation which comes from the energy conservation law. For an ideal beam splitter, the reflectivity of the each side of the beam splitter is different and the incident wave from the direction from the side of lower reflectivity to the side of higher reflectivity of the beam splitter is reflected with the π phase shift or fixed end reflection. This is a simplest choice of the boundary condition at the beam splitter, though one parameter family of the boundary conditions is possible according to the physical property of the beam splitter.
- [13] H. Miao, “Exploring Macroscopic Quantum Mechanics in Optomechanical Devices”, PhD. thesis, The University of Western Australia, 2010.
- [14] The precise meaning of “observe $D_d^\dagger \hat{b}_2 D_d$ ” will be clarified in [15].
- [15] K. Nakamura and M. -K. Fujimoto, arXiv:1709.01697 [quant-ph]; K. Nakamura and M. -K. Fujimoto, arXiv:1711.03713 [quant-ph].

- [16] I. S. Gradshteyn and I. M. Ryzhik, *Table of Integrals, Series, and Products*, 6th ed., edited by A. Jeffrey and D. Zwillinger (Academic, San Diego, 2000).
- [17] F. Quinlan, et al., *Nature photonics*, **7** (2013), 290.